Journal of Power Sources 196 (2011) 2826–2834

Contents lists available at ScienceDirect

Journal of Power Sources

journal homepage: www.elsevier.com/locate/jpowsour

Highly conductive and electrochemically stable plasticized blend polymer electrolytes based on PVdF-HFP and triblock copolymer PPG-PEG-PPG diamine for Li-ion batteries

Diganta Saikia[a], Hao-Yiang Wu[b], Yu-Chi Pan[a], Chi-Pin Lin[a], Kai-Pin Huang[c], Kan-Nan Chen[d], George T.K. Fey[c], Hsien-Ming Kao[a,*]

[a] Department of Chemistry, National Central University, Chung-Li 32054, Taiwan, ROC
[b] Department of Neurological Surgery, Tri-Service General Hospital, National Defense Medical Center, 325, Sec. 2, Cheng-Kung Rd, Taipei 11490, Taiwan, ROC
[c] Department of Chemical and Materials Engineering, National Central University, Chung-Li 32054, Taiwan, ROC
[d] Department of Chemistry, Nano-Tech Research Center, Tamkang University, Tamsui 251, Taiwan, ROC

ARTICLE INFO

Article history:
Received 8 July 2010
Received in revised form
14 September 2010
Accepted 28 October 2010
Available online 3 November 2010

Keywords:
Blend polymer electrolyte
Ionic conductivity
Transference number
Linear sweep voltammetry
Lithium-ion batteries

ABSTRACT

A new plasticized poly(vinylidene fluoride-co-hexafluoropropylene (PVdF-HFP)/PPG-PEG-PPG diamine/organosilane blend-based polymer electrolyte system has been synthesized and characterized. The structural and electrochemical properties of the electrolytes thus obtained were systematically investigated by a variety of techniques including differential scanning calorimetry (DSC), thermogravimetric analysis (TGA), tensile test, Fourier transform infrared spectroscopy (FTIR), ^{13}C and ^{29}Si solid-state NMR, AC impedance, linear sweep voltammetry (LSV) and charge–discharge measurements. The FTIR and NMR results provided the information about the interaction among the constituents in the blend polymer membrane. The present blend polymer electrolyte exhibits several advantageous electrochemical properties such as ionic conductivity up to 1.3×10^{-2} S cm^{-1} at room temperature, high value of Li^+ transference number ($t_+ = 0.82$), electrochemical stability up to 6.4 V vs. Li/Li^+ with the platinum electrode, and stable charge–discharge cycles for lithium-ion batteries.

1. Introduction

The ever increasing pace for the development of storage systems for sustainable energy supplies make the lithium ion battery technology one of the most promising future energy resources as it has tremendous scope to be used in many applications from modern hi-tech devices to hybrid electric vehicles [1–5]. In that context, ion-conducting polymer electrolyte membranes have attracted considerable interests as components for rechargeable lithium-ion batteries [4–16]. General requirements for the membrane materials are high ionic conductivity, good mechanical stability and processing of ultrathin films to allow fast loading processes. Currently, a liquid electrolyte along with a separator is used for fabrication of batteries. However, the possibility of internal shorting, leakage problems and highly reactive nature of such electrolytes towards the electrode surfaces necessitate the protective enclosures, which increase the size of the battery. An ideal way to get a light-weight, leak proof and flexible battery is to use polymer electrolyte serving as a separator as well as an electrolyte. Solid polymer electrolytes (SPEs) have received attention for several decades because they typically possess the mechanical properties and structural integrity required for battery applications [6–10]. However, they have inherently lower conductivities due to the more restricted motion of the polymer molecules and thus make them inadequate for practical use. Due to this reason, much attention has turned to gel or plasticized polymer electrolytes, which can be regarded as an intermediate state between typical liquid electrolytes and dry solid polymer electrolytes [11–15]. Nevertheless, plasticized electrolytes also exhibit drawbacks, such as reactivity of polar solvents with lithium electrode, poor mechanical properties at high degree of plasticization, and solvent volatility.

Polymer blending is another approach to improve the properties of plasticized polymer electrolytes. The main advantages of blend-based polymer electrolytes are simplicity of preparation and easy control of physical properties by changing the composition of blended polymer matrices. In addition, mechanical properties can be controlled in polymer blend systems [16,17]. Typically, the blend polymer electrolyte is composed of at least two polymers, one that absorbs the active elements of the electrolyte and the other that is tougher and comparatively inert, which enhances the mechanical integrity of the blend polymer [18,19]. Among various polymers, poly(vinylidene fluoride-co-hexafluoropropylene (PVdF-HFP) has

* Corresponding author. Tel.: +886 3 4275054; fax: +886 3 4227664.
E-mail address: hmkao@cc.ncu.edu.tw (H.-M. Kao).

0378-7753/$ – see front matter © 2010 Elsevier B.V. All rights reserved.
doi:10.1016/j.jpowsour.2010.10.096

been extensively investigated because of its excellent mechanical strength and electrochemical stability with respect to nonaqueous electrolyte and electrode materials [20–23]. Moreover, the high dielectric constant ($\varepsilon \approx 9.4$–10.6, Aldrich data) and strong electron withdrawing functional group (–C–F–) of PVdF-HFP make it favorable as polymer matrix [24–26].

With the aim of developing a highly conductive polymer electrolyte, herein a triblock copolymer poly(propylene glycol)-*block*-poly(ethylene glycol)-*block*-poly(propylene glycol) bis(2-aminopropyl ether) (PPG-PEG-PPG diamine, H_2N-PPG-PEG-PPG-NH_2, denoted as ED2000) is blended with PVdF-HFP copolymer to synthesize the blend polymer electrolytes. The presence of soft segment in ED2000 (ester carbonyls or ether oxygens) makes it more flexible to trap enough amount of electrolytes. Besides, the PPG segment of ED2000 is miscible with PVdF-HFP [27]. An organosilane plasticizer, 2-methoxy(polyethylenoxy)propyl trimethoxysilane (MPEOP), is also used as the presence of PEG tails in MPEOP helps in the decrease of T_g values [28]. The blending of ED2000 with MPEOP not only improves the miscibility between the organic and inorganic entities, but also guarantees the amorphous behavior of the hybrid electrolytes. Also PEG/PPG part of ED2000 and PEG part of MPEOP may help in the segmental movement of the chain to carry lithium ions. Blending of ED2000 and MPEOP with PVdF-HFP would thus provide a matrix which is flexible as well as mechanically stable. A series of blend polymer electrolytes has been synthesized by varying the weight ratio of PVdF-HFP and ED2000. The structural and electrochemical properties of the electrolytes thus obtained were systematically investigated by a variety of techniques including differential scanning calorimetry (DSC), thermogravimetric analysis (TGA), Fourier transform infrared spectroscopy (FTIR), ^{13}C and ^{29}Si solid-state NMR, AC impedance, linear sweep voltammetry (LSV) and charge–discharge measurements.

2. Experimental

2.1. Preparation of blend polymer electrolytes

The copolymers PVdF-HFP (Aldrich, $M_w = 400{,}000\ g\ mol^{-1}$) and H_2N-$(PPG)_a(PEG)_b(PPG)_c$-NH_2 (Aldrich, $M_w = 2000\ g\ mol^{-1}$, containing $a + c = 3.5$ and $b = 40.5$ units, commercially designated by Jeffamine ED2000) were dried at 70 °C for 24 h under vacuum ($<10^{-3}$ Torr) prior to their use. In a typical synthesis, ED2000 was dissolved in small amount (10 mL) of dried THF and stirred at 60 °C. MPEOP (CH_3O-$(CH_2CH_2O)_n$-$(CH_2)_3Si(OCH_3)_3$, $n = 6$–9, Gelest Inc.) was then added to the above solution and continuously stirred for 2 days at 60 °C. MPEOP, consisting of a PEG segment with an average molecular weight of 375, is uniformly mixed with ED2000 because of its possible interactions with the ED2000 chain. Separately, PVdF-HFP was dissolved in dried THF by stirring at 60 °C. Both the PVdF-HFP and ED2000 solutions were then added together, stirred, and heated at 60 °C for 24 h. The resulting viscous solution thus obtained was cast onto Teflon dishes and the solvent was slowly evaporated at room temperature for 2 days. Finally, the materials were heated at 80 °C under vacuum for another 24 h to get crack-free membranes. This procedure gave homogenous and mechanically strong membranes. The membranes were then stored in a glove box (VAC, MO 40-1) under argon atmosphere for further measurements. The thickness of the membranes was controlled to be in the range of 50–70 μm. Polymer electrolytes were obtained by soaking blend membranes in liquid electrolytes consisting of either 1 M $LiClO_4$ in ethylene carbonate (EC)/propylene carbonate (PC) (1:1, v/v, chemicals obtained from Aldrich) or 1 M $LiPF_6$ in EC/diethyl carbonate (DEC, Tomiyama Chemicals, Japan). The nomenclatures of the blend polymer electrolyte membranes with different compositions in weight ratios are given in Table 1.

2.2. Characterization methods

The blend polymer membrane was dipped in an electrolyte solution of 1 M $LiClO_4$ in EC/PC (1:1, v/v) for measurements of the extent of swelling. The percentage of swelling was determined by $(W - W_0)/W_0 \times 100\%$, where W and W_0 are the weights of the wet and dry blend polymer membrane, respectively. Alternate current (AC) impedance measurements of the blend polymer electrolytes were performed using an Autolab/PGSTAT 302 frequency response analyzer over a frequency range of 10 Hz to 1 MHz with an amplitude of 10 mV. All the specimens were sandwiched by two polished stainless steel blocking electrodes in argon atmosphere inside a glove box for conductivity tests. Scanning electron microscopic (SEM) images were taken on a Hitachi S-3500N electron microscope.

As the lithium perchlorate is a strong oxidizing agent, the use of $LiClO_4$ in battery testing may explode the cell. Because of this safety concern, the electrochemical testing (e.g., LSV and charge–discharge tests) of the cell was carried out with 1 M $LiPF_6$ in EC/DEC as the electrolyte to soak the blend polymer membrane and a standard 2032 coin-cell hardware was used for cell fabrication. The blend polymer membrane was dried overnight at 70 °C in an oven and placed into an argon-filled glove box that contained < 1 ppm oxygen and moisture, to soak in the electrolyte solution for 5 h. The electrochemical stability of the blend polymer electrolytes was determined by LSV using stainless steel (SS) and platinum (Pt) as a working electrode and lithium as counter and reference electrodes for a Li/plasticized blend polymer electrolyte/SS(Pt) cell at a scan rate of $1\ mV\ s^{-1}$ from an open circuit potential to 9 V vs. Li/Li^+. The interfacial resistance between electrolyte and lithium electrode was evaluated by AC impedance method using Autolab/PGSTAT 302 impedance analyzer for a Li/plasticized blend polymer electrolyte/Li symmetric cell. Charge–discharge studies were carried out with Maccor™ multichannel battery tester (S4000). Lithium metal (Alfa Products) was used as the anode. The cathode used commercially available FMC cathode powder of $LiCoO_2$ by blade-coating a slurry of 85 wt.% active material with 10 wt.% conductive carbon black and 5 wt.%

Table 1
Ionic conductivities and percentage of swelling of plasticized blend polymer electrolytes with different compositions.

Sample	Compositions in wt. ratios			Conductivity at 30 °C ($S\ cm^{-1}$)	Swelling (%)
	PVdF-HFP	ED2000	MPEOP		
PED-1	0.5	3.5	0.92	1.1×10^{-2}	229
PED-2	1	3	0.92	1.3×10^{-2}	259
PED-3	2	2	0.92	5.5×10^{-3}	158
PED-4	3	1	0.92	2.8×10^{-3}	102
PED-5	1	3	0	8.3×10^{-3}	186
PED-6	4	0	0.92	1.3×10^{-3}	87
PED-7[a]	1	3	0.92	8.2×10^{-3}	–

[a] Sample is activated with 1 M $LiPF_6$ in EC/DEC, others are activated with 1 M $LiClO_4$ in EC/PC.

poly(vinylidene fluoride) (PVdF) binder in *N*-methyl-2-pyrrolidone (NMP) on aluminum foil, drying overnight at 120 °C in an oven, roller-pressing the dried coated foil, and punching out circular discs. The cycle tests of normal charge were carried out at a 0.2 C-rate between 2.75 and 4.25 V. The Li transference number t_+ was determined by using a combination method of dc polarization and AC impedance measurements, which has been reported by Evans et al. [29] and then modified by Abraham et al. [30]. The current and resistance were measured by an Autolab/PGSTAT 302 impedance analyzer. The sample was assembled in a coin-cell holder using lithium foils as non-blocking electrodes in an argon gas-filled glove box. Finally, it was placed into an oven, which was held the temperature at 70 °C. The dc voltage pulse applied to the cell was 10 mV.

Solid-state NMR experiments were performed on a Varian Infinityplus-500 NMR spectrometer, equipped with a Chemagnetics 7.5 mm probe. The Larmor frequencies for ^{13}C and ^{29}Si nuclei are 125.36 and 99.03 MHz, respectively. ^{29}Si and ^{13}C magic angle spinning (MAS) NMR spectra were acquired at a spinning speed of 5 kHz. The $\pi/2$ pulse length for ^{29}Si nuclei was typically 6 μs. The ^{13}C and ^{29}Si chemical shifts were externally referenced to tetramethylsilane (TMS) at 0 ppm. The ^{13}C cross-polarization magic angle spinning (CPMAS) NMR spectrum was recorded by using a contact time of 1 ms. Mechanical properties of the membranes were evaluated using a QC universal testing machine (Model PT-1066, Taiwan). All the tests were conducted at a crosshead speed of 5 mm min^{-1}.

Differential scanning calorimetry (DSC) was performed in the temperature range from −70 to 250 °C using PerkinElmer Pyris 6 DSC at a heating rate of 10 °C min^{-1}. The sample weights were maintained in the range of 7–8 mg and were hermetically sealed in aluminum pans. The reported DSC curves were the second heating scans taken after an initial heating scan to erase the thermal history, followed by quenching to −70 °C. Thermogravimetric analysis (TGA) was conducted under nitrogen environment at a heating rate of 10 °C min^{-1} from room temperature to 400 °C on a TA instrument Q50 thermogravimetric analyzer. Fourier Transform IR spectra were obtained from a Bio-Rad FTS155 spectrometer over the range of 4000–400 cm^{-1} at a resolution of 4 cm^{-1} using the KBr wafer technique.

3. Results and discussion

3.1. Swelling properties

In order to increase the ionic conductivity, a significant amount of liquid electrolytes is required to be soaked by the polymer membrane in a reasonable short period. Further, the plasticized polymer electrolyte must remain mechanically stable after swelling with liquid electrolytes. Fig. 1 shows the dependence of the percentage of swelling as a function of soaking time for the blend polymer electrolyte system. As shown in Fig. 1, the PVdF-HFP and ED2000 contents have great influence on both uptake rate and percentage of swelling of the blend polymer membranes. In general, the swelling percentage of the blend polymer membranes increased with the soaking time. A maximum percentage of swelling of about 259% was achieved within 30 min of soaking time for the PED-2 sample, which is higher than this kind of blend polymer membranes previously reported [16,17]. The swollen membrane, as shown in the inset of Fig. 1A, was mechanically stable after dipping in the electrolyte solution. Further increasing the ED2000 content in the membrane deteriorated the mechanical property. The higher percentage of swelling suggested the porous structure of the electrolyte membrane. The scanning electron microscopic (SEM) image (inset of Fig. 1B) also confirms the porous structure of the membrane. The swelling rate increased slowly with the increase in the

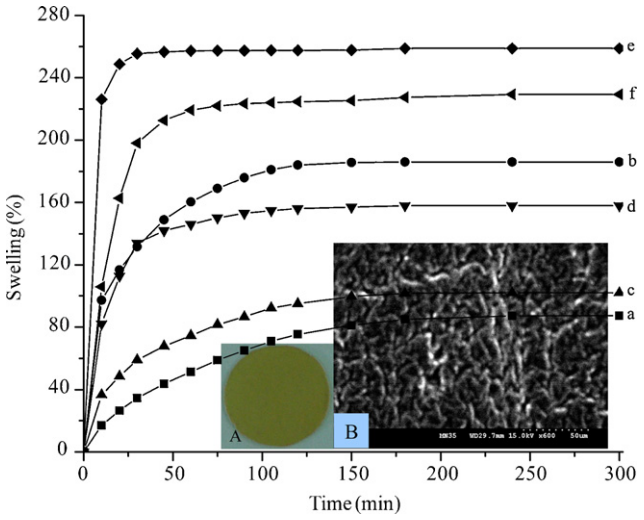

Fig. 1. Swelling behavior of the PVdF-HFP/ED2000/MPEOP blend polymer electrolytes with different weight ratios, (a) 4:0:0.92 (PED-6), (b) 1:3:0 (PED-5), (c) 3:1:0.92 (PED-4), (d) 2:2:0.92 (PED-3), (e) 1:3:0.92 (PED-2) and (f) 0.5:3.5:0.92 (PED-1). The inset figures show the swelled membrane (A) and SEM image of the microporous structure (B).

PVdF-HFP amount and required a longer time to saturate with liquid electrolyte due to the rigid structure of PVdF-HFP. On the other hand, with increasing the ED2000 amount to a certain limit, the blend membrane became more elastic in nature and could absorb a sufficient amount of electrolyte (Table 1). Although the ED2000 amount in PED-1 was larger than in PED-2, its swelling ratio was lower. As the PVdF-HFP amount was less in PED-1 than in PED-2, there was a possibility that the polymer matrix in PED-1 cannot retain the electrolyte proficiently. As a result, the swelling ratio of PED-1 was lower than PED-2. In addition, it was difficult to obtain a stable membrane by increasing the ED2000 amount beyond PED-1 sample since the membrane dissolved in the electrolyte solution. This suggested that ED2000 also has some contribution to enhance electrolyte uptake due to its good affinity with liquid electrolyte. Further, while comparing the PED-5 and PED-2 samples, it was found that the electrolyte uptake was increased with the addition of MPEOP. The EO chain of MPEOP might be helpful in the swelling process as there is a possibility of interaction of EO with liquid electrolyte. This implied that matrix affinity with liquid electrolyte also played an important role in the enhancement of swelling percentage.

3.2. Mechanical property

Fig. 2 shows the stress–strain curves of the solid and plasticized blend polymer membranes as well as for the pure PVdF-HFP membrane. As seen in Fig. 2, the mechanical properties of these blend membranes depend on the composition ratios. The blend membranes show higher yield stress than the pure PVdF-HFP membrane except PED-2 and PED-5. Moreover, the elongations of all the blend membranes are larger than that of the pure PVdF-HFP membrane, which suggests good elastic properties of the membranes. Both the stress and strain for solid blend polymer membranes increase with the increase in the PVdF-HFP amount. On the other hand, the addition of ED2000, which contains soft segments in the polymer chain, helps in the elongation of the blend polymer membranes. The blend membrane PED-6 that contains PVdF-HFP and MPEOP shows high strength as well as elongation. The presence of alkoxysilane group in MPEOP might help in the enhancement of stress–strain behavior of the membrane. For the case of plasticized electrolyte (soaking with 1 M $LiClO_4$ in EC/PC (1:1, v/v))

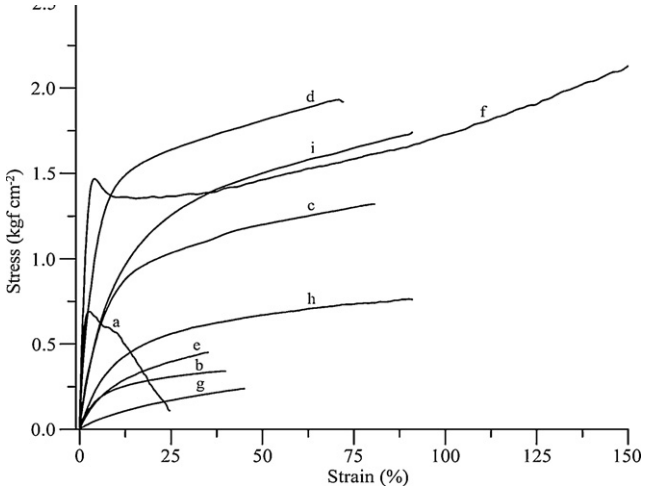

Fig. 2. Stress–strain curves of blend polymer membranes (a) pure PVdF-HFP, (b) solid PED-2, (c) solid PED-3, (d) solid PED-4, (e) solid PED-5, (f) solid PED-6, (g) plasticized PED-2, (h) plasticized PED-3 and (i) plasticized PED-4.

membranes of PED-2, PED-3 and PED-4, their elongations are larger than the solid counterparts although the electrolyte membranes show lower fracture strength than the solid membranes. The electrolyte trapped inside the pores of the membrane makes it more elastic in nature but reduces the yield stress. Therefore, the plasticized blend polymer electrolyte membranes are more ductile than the solid blend polymer membranes. The results suggest that the PVdF-HFP-ED2000-MPEOP blend polymer membranes have good property of elongation, which are beneficial in the fabrication of polymer lithium ion batteries.

3.3. ^{13}C and ^{29}Si solid-state NMR

Solid-state ^{13}C CPMAS NMR experiment was performed to obtain the backbone structure of the blend polymer membrane. Fig. 3 shows the ^{13}C CPMAS NMR spectrum of the blend polymer membrane acquired at a short contact time of 1.0 ms. The most predominant peak at 70.1 ppm is assigned to methylene carbons adjacent to the ether oxygens of the polymer chain [9]. Because of the high concentration of these moieties in ED2000, the signals associated with the carbon atoms of all the other functional groups present in this matrix are relatively weak. The methyl carbon from the propylene oxide units appears at 16.8 ppm, while the peak at 43.2 ppm can be assigned to the methylene carbons in PVdF-HFP. The small peak around 164 ppm is assigned to the carbon atom

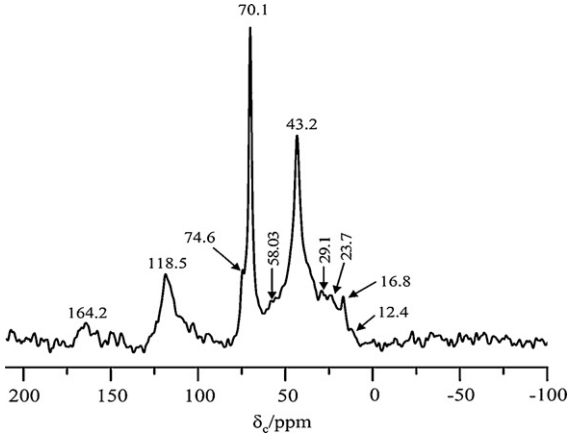

Fig. 3. ^{13}C CPMAS NMR spectra of PED-2 blend polymer membrane.

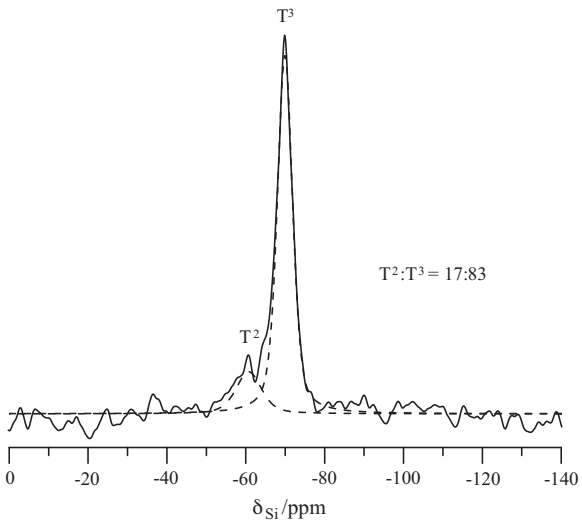

Fig. 4. ^{29}Si MAS NMR spectra of PED-2 membrane. The dashed lines represent the components used for the spectral deconvolution.

attached to the $-CF_3$ group of PVdF-HFP and the peak at 118.5 ppm is due to the carbon atom of CF_2. The peak at 29.1 ppm is ascribed to the methylene carbon attached to the methoxy group of MPEOP. Two small peaks at 23.7 and 12.4 ppm are assigned to the methylene carbons in α and β positions to the silicon atom of MPEOP, respectively. Besides the major peak at 70.1 ppm, there is a smaller peak at 74.6 ppm due to the ether carbons in the PPG segments of ED2000, which is also clearly resolved for the parent ED2000. A small peak around 58 ppm is due to the non-hydrolyzed ethoxy groups in organosilanes.

The condensation degree of the silica network architecture inside the materials can be directly characterized by using ^{29}Si MAS NMR. As shown in Fig. 4, a dominant signal at −70 ppm, corresponding to T^3 ($RSi(OSi)_3$, where R refers to an alkyl group) and a small peak around −61 ppm corresponding to T^2 ($RSi(OSi)_2(OH)$) sites, were observed. The observation of T groups indicated the presence of organosilane in the material. This organosilane (i.e., MPEOP) was stable under synthesis conditions since the Si–C cleavage was not observed due to the formation of Q ($Si(OSi)_4$) groups.

3.4. Thermal stability

Fig. 5A shows the DSC curves of the PED-2 blend polymer membrane, along with the parent ED2000 for comparison purposes. The sharp peak observed around 28 °C is due to the melting of ED2000 [31]. After plasticization with 1 M $LiClO_4$ in EC/PC, this peak disappeared, indicating that the plasticized sample was amorphous in nature (part b of Fig. 5A). Rather, two new peaks appeared around 75 °C and 210 °C. The peak around 75 °C might be due to some impurities (e.g., water) present in the sample. The peak around 210 °C was probably due to the overlap of the boiling points of EC (260 °C) and PC (240 °C). No melting peak (∼140 °C) was observed for PVdF-HFP, indicating that PVdF-HFP remained amorphous in the resulting blend polymer electrolytes [13]. As the melting transition of both ED2000 and PVdF-HFP was absent from the blend polymer electrolyte sample, it was concluded that both the polymers were miscible with each other and their interactions led to reduction in crystallinity of the electrolyte membrane.

The TGA curve of the PED-2 blend polymer membrane is shown in Fig. 5B. There is no obvious weight loss until the temperature is higher than 150 °C. Therefore, the membrane is thermally stable at least up to 150 °C and suitable as a separator for Li-ion batteries within this temperature limit.

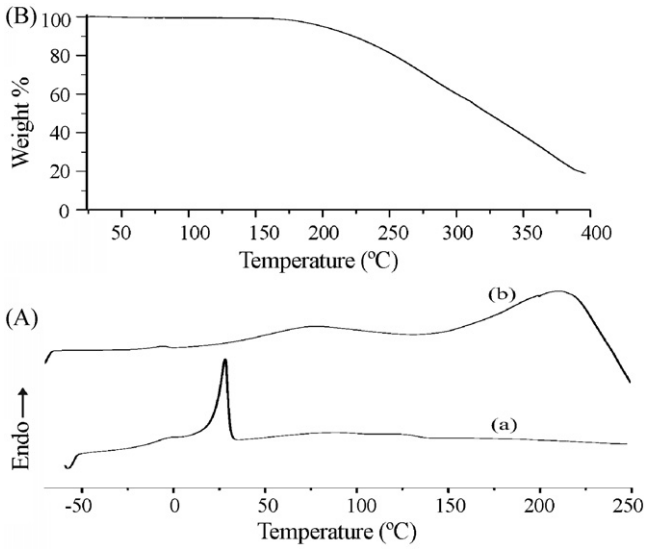

Fig. 5. (A) DSC thermograms of (a) pure ED2000 and (b) PED-2 blend polymer membrane. (B) TGA curve of PED-2.

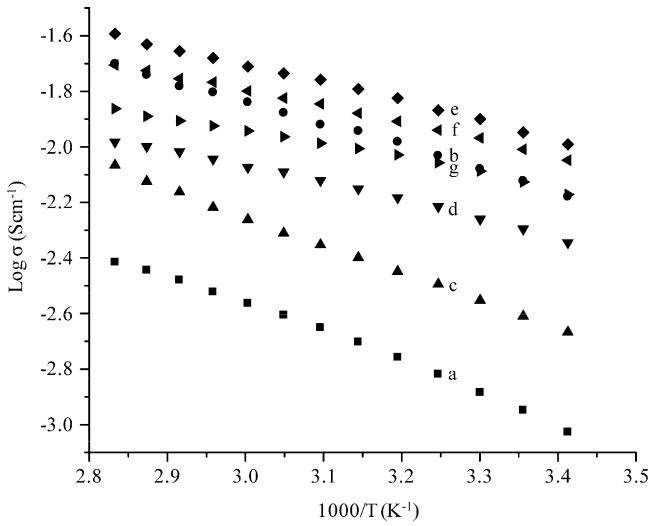

Fig. 7. Temperature dependence of ionic conductivity of PVdF-HFP/ED2000/MPEOP blend polymer electrolytes with different weight ratios, (a) 4:0:0.92 (PED-6), (b) 1:3:0 (PED-5), (c) 3:1:0.92 (PED-4), (d) 2:2:0.92 (PED-3), (e) 1:3:0.92 (PED-2), (f) 0.5:3.5:0.92 (PED-1), and (g) the sample (e) with 1 M $LiPF_6$ in EC/DEC (PED-7).

3.5. FTIR

Infrared spectroscopy was used to characterize the chain structure of the blend polymer membrane. The complexation between the blend polymer components can either shift or diminish intensities in the polymer peak frequencies. Fig. 6 shows the FTIR spectra of pure ED2000, pure PVdF-HFP and the PED-2 blend polymer membrane. The band at 3476 cm^{-1} in pure ED2000 was assigned to hydrogen-bonded N–H stretching mode [32]. The intensity of this band was decreased after complexation with PVdF-HFP and MPEOP in the blend membrane. The peak at 2876 cm^{-1}, which was due to CH_2 stretching vibration of EO chain of ED2000, shifted to 2870 cm^{-1} in the blend membrane. As MPEOP also has the EO chain, vibration of CH_2 band of MPEOP is expected to appear at the same frequency. The band at 1653 cm^{-1} in pure ED2000 which was shifted to 1671 cm^{-1} in the blend membrane was attributed to C–N stretching vibration [33]. Another C–N stretching vibrational band was also observed at 1249 cm^{-1} in the blend polymer. The bands at 1456 and 1349 cm^{-1} were due to CH_2 scissoring and wagging vibration of the polymer. A major band associated with C–O stretching vibrations was observed at 1107 cm^{-1} for the parent ED2000 and the blend polymer membrane. This band shifted slightly towards lower frequency for the blend polymer membrane. It is attributed to the specific interaction between the fluorine in PVdF-HFP and the carbon connected to oxygen of ED2000, which can act as a Lewis base and a Lewis acid, respectively [27,34]. A band at 950 cm^{-1} with a medium intensity was assigned to the coupled vibration of C–C stretching and CH_2 rocking modes [35]. There is a strong possibility of Si–OH present in the blend membrane due to MPEOP which overlaps with the band frequency at 950 cm^{-1}. The presence of Si–OH groups in the blend polymer was also confirmed by the observation of T^2 species in the ^{29}Si NMR spectrum (Fig. 4). The other bands at 1287, 882 and 842 cm^{-1} for the blend membrane are related to PVdF-HFP. As seen in Fig. 6b, both α and β phase of the PVdF-HFP are present in the pure sample. The bands at 531, 613, 796, 975 and 1401 cm^{-1} corresponding to the α phase of PVdF are absent in the blend polymer membrane. Rather, we observed the bands at 842, 880 and 1287 cm^{-1} belonging to the β phase of PVdF [36] in the blend membrane. This suggests that the highly ordered spherulitic structure of α phase is diminished or converted to fibrous β phase in the blend polymer membrane. The bands at 1287 and 882 cm^{-1} are assigned to the C–F and–CF_2 stretching of PVdF-HFP, respectively. The bands due to CH_2 rocking vibration of both PVdF-HFP and EO chain were observed at 842 cm^{-1}. The appearance of only fibrous β phase of PVdF-HFP in the blend polymer membrane paved the way for higher conductivity due to its lower crystallinity. In comparison to the pure components used in the blend polymer, the significant changes in the band positions and/or in the band magnitude of the blend polymer indicates that there are some interactions among ED2000, MPEOP and PVdF-HFP.

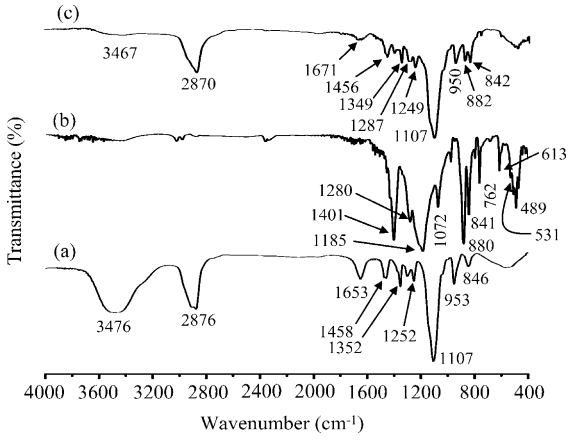

Fig. 6. FTIR spectra of (a) pure ED2000, (b) pure PVdF-HFP and (c) PED-2 blend polymer membrane.

3.6. Ionic conductivity

The temperature dependence of ionic conductivities of the blend polymer electrolytes with different weight ratios of PVdF-HFP and ED2000 are shown in Fig. 7. The electrolyte shows an Arrhenius-like enhancement of conductivity when the temperature is increased, indicating that ion transport is mainly decoupled from the polymer segmental motion. The variation of ionic conductivity with different weight ratios of the constituents are extensively studied using 1 M $LiClO_4$ in EC/PC and particularly for the PED-7 sample with 1 M $LiPF_6$ in EC/DEC. The room temperature ionic conductiv-

ity and percentage of swelling with different compositions of the blend polymer electrolytes are listed in Table 1. As expected, the ionic conductivity increased with the increased in swelling percentage. On the other hand, the ionic conductivity decreased with the increased in PVdF-HFP amount for the present blend electrolyte system (Table 1). At lower amounts of PVdF-HFP (e.g., 0.5 and 1 g), the conductivity values are nearly identical and a maximum ionic conductivity value of 1.3×10^{-2} S cm^{-1} at 30 °C is obtained for the PED-2 sample, which is remarkably high for plasticized blend polymer electrolytes and comparable with the conductivity of liquid electrolytes. As the amount of PVdF-HFP increased in the membrane composition, it is anticipated that the rigid structure of PVdF-HFP prevented the swelling of the membrane. As evident from Table 1, the ionic conductivity increased with the increased in ED2000 contents. Without the addition of ED2000, the conductivity decreases to its lowest value of 1.3×10^{-3} S cm^{-1} at 30 °C, which is one order of the magnitude lower than the maximum value. Thus, it can be concluded that ED2000 helps in the uptake of liquid electrolyte to enhance ionic conductivity. Besides, the conductivity of PED-5, a sample without addition of MPEOP, only reaches 8.3×10^{-3} S cm^{-1} at 30 °C, which is slightly lower than the maximum conductivity value. This suggests that the MPEOP behaves more like a plasticizer as the PEG chain of the MPEOP helps to provide a large free volume for the rapid movement of ions to enhance the ionic conductivity.

The higher ionic conductivity obtained in the present blend electrolyte is attributed to the porous structure of the membrane (Fig. 1B), which helps to uptake more electrolytes. In addition, the interconnected pores formed between spherulites, which act like channels for lithium ion movement, helps further enhancement in ionic conductivity. In the membranes with high electrolyte uptakes (swelling percentage), these interconnected pore channels are filled with liquid electrolytes, and thus Li^+ ion can move faster through these channels to give higher ionic conductivity.

According to the previous studies [37,38], the liquid electrolytes were entrapped in the pores of the polymer matrix and then penetrated into the polymer chains for swelling the amorphous domains. Lithium ions can transfer in three ways within the porous polymer electrolyte: through liquid electrolyte stored in the pores, amorphous domains swelled by liquid electrolyte and along the polymer chains. The transfer of lithium ions along polymer chains was much slower than transfer through pores and amorphous domains. The Arrhenius behavior of conductivity for the present system also ruled out the possibility of segmental movement of ions was the main cause of ion transport. Therefore, the pores filled with liquid electrolyte and swelled amorphous domains were the main transfer channels of lithium ions. Both factors significantly contributed to the ionic conductivity. The porosity, amorphous domains, ED2000 content and MPEOP made the blend membrane capable of higher electrolyte uptake, which in turn increased the concentrations of lithium ions, leading to enhancement of ionic conductivity.

To compare the two liquid electrolytes, the PED-2 sample, which gave the highest ionic conductivity with 1 M $LiClO_4$ in EC/PC, was also tested with 1 M $LiPF_6$ in EC/DEC (PED-7). A conductivity value of 8.2×10^{-3} S cm^{-1} at 30 °C was obtained for PED-7. The lower ionic conductivity of the membrane with $LiPF_6$ salt is attributed to the low dielectric constant of DEC ($\varepsilon = 2.82$) in comparison to PC ($\varepsilon = 64.4$). The dielectric constant of binary solvent mixture of EC ($\varepsilon = 89$)/PC is about 76.7 and EC/DEC is 45.9 [39,40]. The solvents with high dielectric constants dissociate the lithium salts more easily into free Li^+ ions and thus help in the enhancement of ionic conductivity. As a result, the conductivity is higher in the blend polymer membrane plasticized with 1 M $LiClO_4$ in EC/PC in comparison to that plasticized with 1 M $LiPF_6$ in EC/DEC.

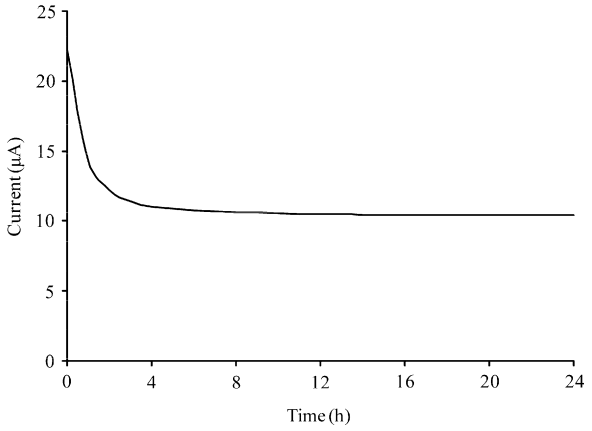

Fig. 8. Depolarization curve of plasticized PED-7 blend polymer electrolyte.

3.7. Transference number measurements

The lithium ion transference number, t_+, is an important parameter for rechargeable lithium ion batteries [29,30]. A relatively high t_+ can eliminate the concentration gradients within the battery and ensure the battery operation under a high current density [41]. The equations used by Evans and Abraham are shown in Eqs. (1) and (2), respectively.

$$t_+ = \frac{I_s(\Delta V - I_0 R_0)}{I_0(\Delta V - I_s R_s)} \quad (1)$$

$$t_+ = \frac{I_s R_{b,s}(\Delta V - I_0 R_0)}{I_0 R_{b,0}(\Delta V - I_s R_s)} \quad (2)$$

where ΔV is the potential applied across the cell. I_0 and I_s are the initial and steady-state dc currents, $R_{b,0}$ and $R_{b,s}$ are the initial and final resistances of the electrolytes, and R_0 and R_s are the initial and steady-state resistances of the passivating layers. The sample is subjected to a small dc polarization potential (10.0 mV) for sufficient time to obtain a steady-state current. The bulk electrolyte and interfacial resistances of the cell are measured before and after polarization by ac impedance. As the ionic conductivity reaches the maximum value in the PED-2 sample, we have measured the Li^+ transference number for PED-7 (same sample composition but with 1 M $LiPF_6$ in EC/DEC) sample. Due to explosive nature of $LiClO_4$, 1 M $LiPF_6$ in EC/DEC was used as an electrolyte to plasticize the blend polymer membrane for all the testing using the lithium metal as electrode element. The depolarization curve of the plasticized PED-7 blend polymer electrolyte is shown in Fig. 8. The initial current was 22.2 μA and finally reached 10.4 μA, leading to a Li^+ transference number of 0.74, which is a remarkably high value in comparison to other blend-based polymer electrolytes [16,42]. The Abraham method takes into account of the change in bulk electrolyte resistance ($R_{b,0} = 4.6\ \Omega$ and $R_{b,s} = 5.1\ \Omega$), which is generally small, but has some definitive effects on transference number. With the Abraham method, the Li^+ transference number is measured to be 0.82. Therefore it is clear that a large proportion of current is carried by lithium ions in this blend polymer electrolyte. The high value of the Li^+ transference number is attributed to the higher electrolyte retention capability of the blend polymer due to its porous structure. Higher percentage of liquid electrolyte entrapment inside the pores creates electrolyte channels within the polymer matrix, through which the lithium ions can move faster and facilitates a higher transference number. Besides, the formation of silica domains within the matrix is evidenced in the ^{29}Si NMR spectrum due to the presence of MPEOP. The surface of these silica domains may act as Lewis acid and interact with the oxygen

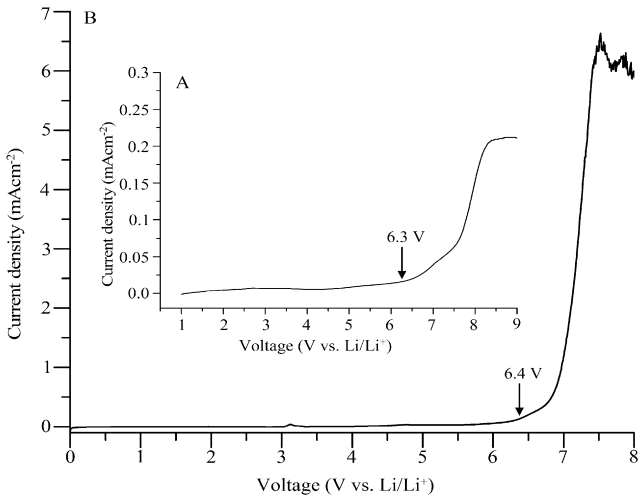

Fig. 9. Linear sweep voltammetry curve of the cell prepared with plasticized PED-7 blend polymer electrolyte, (A) with SS electrode and (B) with Pt electrode.

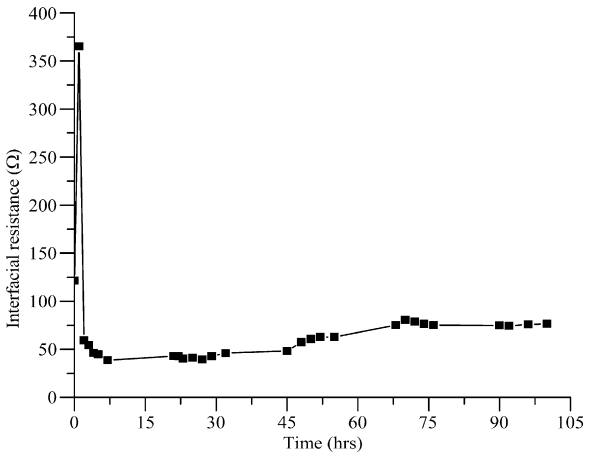

Fig. 10. Variation of interfacial resistance as a function of time for the Li/PED-7/Li symmetric cell kept at 5 V at 25 °C.

atoms of PEG-PPG (Lewis base) chain of ED2000 and hence weaken the interactions between these O atoms and Li^+ [43]. As a result, more free Li^+ ions are released which contributed to the higher Li^+ transference number. The higher transference number supports the higher ionic conductivity result of the blend polymer electrolyte.

3.8. Linear sweep voltammetry

The electrochemical stability of the plasticized blend polymer electrolyte was investigated by linear sweep voltammetry to endure the operating voltage of the battery system, and its corresponding voltammogram is shown in Fig. 9. A very low background current was measured in a potential region between 0 and 6.3 V for the cell prepared with SS electrode. This small current might be attributed to the change of the stainless steel surface [44]. Upon reaching around 6.3 V, a considerable current began to flow, indicating the onset of the electrolyte decomposition process. Therefore, the onset decomposition voltage of the blend polymer electrolyte is around 6.3 V vs. Li/Li^+ with the SS electrode. To verify the stability limit, the LSV measurement was repeated with a more stable electrode platinum (Pt) by replacing the SS electrode. It was observed that the stability window of the blend polymer electrolyte was slightly extended to around 6.4 V with the platinum electrode. The small hump around 3 V in the platinum electrode cell is ascribed to the oxidation of some trace species such as water and oxygen [45]. The oxidation potential reported here is relatively higher compared to the common values of potentials of around 4–5.5 V reported for other polymer electrolytes [16,42,46,47]. The obtained high value of oxidation potential may depend on various factors. It is reported that PVdF-HFP based polymer electrolytes are highly anodically stable because of the presence of strong electron withdrawing functional group (–C–F) [5]. The formation of silica domain in polymer electrolyte could also help in the extension of oxidation potential [48]. The silica domain may trap the traces of residual impurities and shield the lithium from corrosion. The presence of silanol groups (Si–OH), as evidenced from IR and ^{29}Si NMR measurements, suggests that Si–OH could form a thin protective layer on lithium electrode and prevents the electrolyte decomposition, leading to enhancement in the electrochemical stability. Besides, liquid electrolyte is absorbed efficiently by the blend polymer membrane and there may be no separate electrolyte leakage which can react with Li to reduce the stability. All these factors effectively act on the blend polymer electrolyte system and enhance the oxidation potential to such a high level. The present investigation suggests that the synthesized blend polymer electrolyte could be suitable for the high voltage cathode materials with Li intercalation.

3.9. Interfacial resistance

The interfacial resistance plays a crucial role in determining shelf life, safety, lithium deposition and dissolution efficiency, and cycle life of a battery [49]. Uncontrolled passivation phenomena affect the lithium electrode which may lead to serious safety hazards. Therefore, the criteria for the selection of a proper battery electrolyte must be based not only on fast transport properties but also on favorable interfacial properties [49,50]. In the present study, the stability of the lithium interface is examined by measuring the interfacial resistance. Fig. 10 shows the variation of interfacial resistance (R_i) as a function of time keeping the lithium electrodes at 5 V. It is observed that the growth of interfacial resistance does not follow a regular trend. The interfacial resistance increases initially for 1 h and then decreases to a certain level and maintains that up to 29 h. It again starts increasing slowly up to 70 h and then slightly decreases and almost constant up to 100 h. The presence of lithium salt, trace amounts of water and synthesis or processing residues may contributes to the observed instability of the lithium anode–polymer electrolyte interface. An increase of R_i with time may be related to a resistive layer continuously growing on the lithium electrode surface, i.e., lithium electrode is passivated when in contact with the blend polymer electrolyte [51]. The passivation of film may be caused by the ethylene carbonate (EC) which is used as plasticizer in the electrolyte component and well known lithium corrosive agent [52]. As a result, the passivated film may contain all the products of unexpected reactions of lithium electrodes with ethylene carbonate and the carbonyl groups on the polymer chains. The other possible reason of the increase in R_i could be the contact problem. With changing morphology of the passivation layer, it is likely that the plasticized blend polymer electrolyte could be partly peeled off from the Li electrodes. The irregular variation of R_i can be ascribed to the change in passivation film morphology with time to finally acquire a non-compact, possibly porous structure [53].

3.10. Charge–discharge behavior

Fig. 11 shows the first cycle charge–discharge behavior of the Li/PED-7/$LiCoO_2$ cell between 2.75 and 4.25 V at a scan rate of

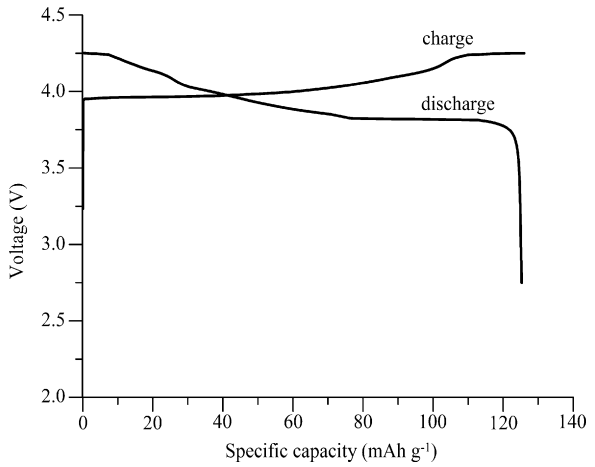

Fig. 11. Galvanostatic first cycle charge–discharge curve for the Li/PED-7/$LiCoO_2$ cell.

0.2 C. The cut-off voltage was selected to prevent destroying of the crystallinity of $LiCoO_2$. It was observed that cycle stability and initial capacity declined slowly, which could be attributed to the formation of a solid electrolyte interface (SEI) film that resulted in significant impedance growth. The cell delivered a coulombic efficiency of 99.4% and 98.7% for the 1st and 25th cycles, respectively. The discharge capacity as a function of cycle number of the cell using PED-7 blend polymer electrolyte as a separator is shown in Fig. 12. The theoretical capacity of the $LiCoO_2$ electrode is 120 mAh g^{-1}. The initial discharge capacity of the present cell is 125 mAh g^{-1} and decreases gradually with subsequent cycling, which is due to the formation of Li/polymer electrolyte interface layer [54]. At 60 cycles, about 86% of the initial discharge capacity is retained without any sign of cell failure. During the cycling, the physical changes in the active materials and the passivation film on the surface of the electrode gradually increase cell internal resistance and block the charge transfer reaction between the Li electrode and the blend polymer electrolyte which results in the discharge capacity loss with cycling. As the capacity loss is only 14% up to 60 cycles, it implies that a good compatibility between blend polymer and liquid electrolyte makes the blend polymer electrolyte retain the liquid electrolyte very efficiently.

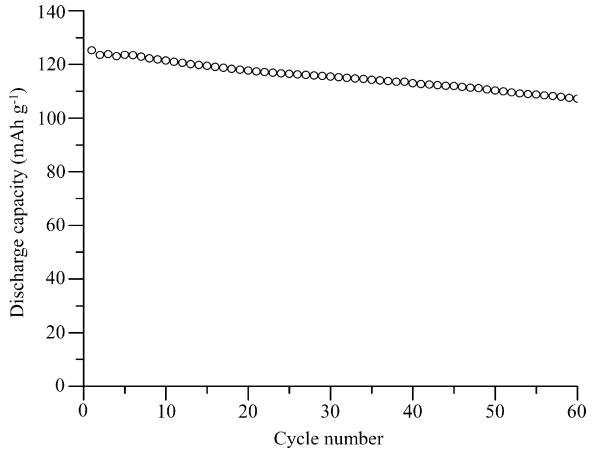

Fig. 12. Cycling behaviors of the Li/PED-7/$LiCoO_2$ cell. The charge–discharge process was performed between 2.75 and 4.25 V at a scan rate of 0.2 C.

4. Conclusions

A highly conductive and electrochemically stable blend polymer electrolyte based on PVdF-HFP, PPG-PEG-PPG diamine and MPEOP has been synthesized. The blend electrolytes exhibited a remarkable swelling ratio and required only 30 min to activate the membrane with electrolyte solution for the best composition. The plasticized membrane shows high value of ionic conductivity about 10^{-2} S cm^{-1}, electrochemical stability window of about 6.4 V vs. Li/Li^+ with the platinum electrode and almost stable discharge capacity with cycle numbers, which make it very promising for lithium ion battery applications.

Acknowledgment

The financial support of this work by the National Science Council of Taiwan is gratefully acknowledged.

References

[1] C.A. Vincent, B. Scrosati, Modern Batteries: An Introduction to Electrochemical Power Sources, Butterworth-Heinemann, London, 1997.
[2] M. Armand, J.-M. Tarascon, Nature 451 (2008) 652–657.
[3] A.M. Christie, S.J. Lilley, E. Staunton, Y.G. Andreev, P. Bruce, Nature 433 (2005) 50–53.
[4] F.M. Gray, Solid Polymer Electrolytes: Fundamentals and Technological Applications, VCH, New York, 1991.
[5] J.Y. Song, Y.Y. Wang, C.C. Wan, J. Power Sources 77 (1999) 183–197.
[6] D.E. Fenton, J.M. Parker, P.V. Wright, Polymer 14 (1973) 589.
[7] P.V. Wright, Br. Polym. J. 7 (1975) 319–327.
[8] M. Marzantowicz, J.R. Dygas, F. Krok, A. Tomaszewska, Z. Florjańczyk, E. Zygadło-Monikowska, G. Lapienis, J. Power Sources 194 (2009) 51–57.
[9] H.-M. Kao, T.-T. Hung, G.T.K. Fey, Macromolecules 40 (2007) 8673–8683.
[10] P.C. Barbosa, M.M. Silva, M.J. Smith, A. Gonçalves, E. Fortunato, S.C. Nunes, V. de Zea Bermudez, Electrochim. Acta 54 (2009) 1002–1009.
[11] H.S. Min, J.M. Kim, D.W. Kim, J. Power Sources 119 (2003) 469–472.
[12] W. Pu, X. He, L. Wang, Z. Tian, C. Jiang, C. Wan, J. Membr. Sci. 280 (2006) 6–9.
[13] D. Saikia, A. Kumar, Electrochim. Acta 49 (2004) 2581–2589.
[14] C.S. Kim, S.M. Oh, Electrochim. Acta 46 (2001) 1323–1331.
[15] J.-H. Cao, B.-K. Zhu, Y.-Y. Xu, J. Membr. Sci. 281 (2006) 446–453.
[16] A. Subramania, N.T. Kalyana Sundaram, A. Rohini Priya, R. Gangadharan, T. Vasudevan, J. Appl. Polym. Sci. 98 (2005) 1891–1896.
[17] Z.L. Wang, Z.Y. Tang, Electrochim. Acta 49 (2004) 1063–1068.
[18] I. Nicotera, L. Coppola, C. Oliviero, M. Castriota, E. Cazzanelli, Solid State Ionics 177 (2006) 581–588.
[19] Z. Tian, W. Pu, X. He, C. Wan, C. Jiang, Electrochim. Acta 52 (2007) 3199–3206.
[20] N.K. Chung, Y.D. Kwon, D. Kim, J. Power Sources 124 (2003) 148–154.
[21] Y. Ding, P. Zhang, Z. Long, Y. Jiang, F. Xu, W. Di, J. Membr. Sci. 329 (2009) 56–59.
[22] Z. Ren, Y. Liu, K. Sun, X. Zhou, N. Zhang, Electrochim. Acta 54 (2009) 1888–1892.
[23] A.M. Stephan, K.S. Nahm, T.P. Kumar, M.A. Kulandainathan, G. Ravi, J. Wilson, J. Power Sources 159 (2006) 1316–1321.
[24] C.Y. Chiang, Y.J. Shen, M.J. Reddy, P.P. Chu, J. Power Sources 123 (2003) 222–229.
[25] N.S. Mohamed, A.K. Arof, J. Power Sources 132 (2004) 229–234.
[26] C.L. Cheng, C.C. Wan, Y.Y. Wang, Electrochem. Commun. 6 (2004) 531–535.
[27] C.G. Wu, M.I. Lu, H.J. Chuang, Polymer 46 (2005) 5929–5938.
[28] L.M. Bronstein, R.L. Karlinsey, K. Ritter, C.G. Joo, B. Stein, J.W. Zwanziger, J. Mater. Chem. 14 (2004) 1812–1820.
[29] J. Evans, C.A. Vincent, P.G. Bruce, Polymer 28 (1987) 2324–2328.
[30] K.M. Abraham, Z. Jiang, B. Carroll, Chem. Mater. 9 (1997) 1978–1988.
[31] H.-M. Kao, S.-W. Chao, P.-C. Chang, Macromolecules 39 (2006) 1029–1040.
[32] D. Saikia, H.-Y. Wu, Y.-C. Pan, C.-C. Liao, C.-F. Chen, G.T.K. Fey, H.-M. Kao, Electrochim. Acta 54 (2009) 7156–7166.
[33] T. Miyazawa, T. Shimanouchi, S.-I. Mizushima, J. Chem. Phys. 24 (1956) 408–418.
[34] Y.J. Wang, D. Kim, J. Power Sources 166 (2007) 202–210.
[35] M.M. Silva, V. de Zea Bermudez, L.D. Carlos, A.P.P. de Almeida, M.J. Smith, J. Mater. Chem. 9 (1999) 1735–1740.
[36] C.-H. Du, B.-K. Zhu, Y.-Y. Xu, J. Mater. Sci. 41 (2006) 417–421.
[37] Y. Saito, H. Kataoka, E. Quartarone, P. Mustarelli, J. Phys. Chem. B 106 (2002) 7200–7204.
[38] Z.H. Li, G.Y. Su, X.Y. Wang, D.S. Gao, Solid State Ionics 176 (2005) 1903–1908.
[39] M. Kumar, S.S. Sekhon, Ionics 8 (2002) 223–233.
[40] R. Kumar, B. Singh, S.S. Sekhon, J. Mater. Sci. 40 (2005) 1273–1275.
[41] J.M. Tarascon, M. Armand, Nature 414 (2001) 359–367.
[42] M. Sivakumar, R. Subadevi, S. Rajendran, H.-C. Wu, N.-L. Wu, Eur. Polym. J. 43 (2007) 4466–4473.
[43] J. Xi, X. Tang, Electrochim. Acta 50 (2005) 5293–5304.
[44] D.Y. Zhou, G.Z. Wang, W.S. Li, G.L. Li, C.L. Tan, M.M. Rao, Y.H. Liao, J. Power Sources 184 (2008) 477–480.

[45] Y.X. Jiang, Z.F. Chen, Q.C. Zhuang, J.M. Xu, Q.F. Dong, L. Huang, S.G. Sun, J. Power Sources 160 (2006) 1320–1328.
[46] W. Li, M. Yang, M. Yuan, Z. Tang, J.Q. Zhang, J. Appl. Polym. Sci. 106 (2007) 3084–3090.
[47] C.G. Wu, M.I. Lu, C.C. Tsai, H.J. Chuang, J. Power Sources 159 (2006) 295–300.
[48] J. Zhou, P.S. Fedkiw, S.A. Khan, J. Electrochem. Soc. 149 (2002) A1121–A1126.
[49] J. Kuratomi, T. Iguchi, T. Bando, Y. Aihara, T. Ono, K. Kuwana, J. Power Sources 97/98 (2001) 801–803.
[50] K. Kanamura, H. Tamura, S. Shiraishi, Z. Takehara, J. Electrochem. Soc. 142 (1995) 340–347.
[51] M. Kono, M. Nishiura, E. Ishiko, J. Power Sources 81/82 (1999) 748–751.
[52] K.-H. Lee, Y.-G. Lee, J.-K. Park, D.-Y. Seung, Solid State Ionics 133 (2000) 257–263.
[53] G.B. Appetecchi, F. Croce, B. Scrosati, Electrochim. Acta 40 (1995) 991–997.
[54] H.-H. Kuo, W.-C. Chen, T.-C. Wen, A. Gopalan, J. Power Sources 110 (2002) 27–33.